Electrochemical measurements of LiF-CaF2-ThF4 melt and activity coefficient of ThF4 in LiF-CaF2 eutectic melt

P. Souček, D. Rodrigues, O. Beneš, S. Delpech, A. Rodrigues, R.J.M. Konings

Electrochimica Acta 380 (2021) 138198

Contents lists available at ScienceDirect

Electrochimica Acta

journal homepage: www.elsevier.com/locate/electacta

Electrochemical measurements of LiF-CaF_2-ThF_4 melt and activity coefficient of ThF_4 in LiF-CaF_2 eutectic melt

P. Souček[a,*], D. Rodrigues[a,b], O. Beneš[a], S. Delpech[b], A. Rodrigues[a], R.J.M. Konings[a]

[a] European Commission, Joint Research Centre, P.O. Box 2340, Karlsruhe 76125, Germany
[b] IJCLab, Univ. Paris-Saclay, Orsay Cedex 91405, France

ARTICLE INFO

Article history:
Received 1 October 2020
Revised 18 March 2021
Accepted 19 March 2021
Available online 25 March 2021

Keywords:
Molten salt reactor
Electrochemical measurement of ThF_4
activity coefficient
Electrochemistry of ThF_4
Eutectic LiF-CaF_2 molten salt
Eutectic LiF-ThF_4 molten salt

ABSTRACT

Thermodynamic and electrochemical properties of actinides in molten fluoride salts are one of the key data required for design and safety assessment of any molten salt reactor concept using liquid fluoride based fuel. In the case of the Molten Salt Fast Reactor (MSFR), special attention has to be paid to thorium fluoride, which is a direct fuel carrier salt constituent. This work presents experimental measurement of ThF_4 activity coefficient in eutectic LiF-CaF_2 melt by electrochemical techniques. The proposed approach is overcoming problems related to the lack of a thermodynamic reference electrode for high-temperature molten fluoride media. The method can be used to compare stability of fissile material and fission products in a given molten fluoride solvent by estimating their activity coefficients using the described electrochemical measurements. In addition, electrochemical methods were successfully used to evaluate and confirm purity of the used materials, with a special regard to oxygen content in the ThF_4 input material synthesised during the previous work from ThO_2.

1. Introduction

A worldwide increased interest in the molten salt reactor (MSR) technology has resulted in the inclusion of this concept amongst the six innovative reactors studied by the Generation IV initiative since 2001 [1]. The Molten Salt Fast Reactor (MSFR) is one of the concepts studied, the design of which was made by CNRS, France, and further developed since 2004 [2–6]. Since 2015, safety aspects of the MSFR have been studied through European EC/EURATOM projects SAMOFAR [7,8] and SAMOSAFER [9]. In the MSFR concept, the fissile material is dissolved in a molten fluoride salt media, which circulates in the core and serves both as fuel and primary circuit coolant. The reactor can be operated as a breeder using Th/U fuel cycle or as an incinerator burning transuranium elements (TRU) [10]. The fuel salt is composed of an eutectic carrier melt LiF-ThF_4 (78.0–22.0 mol.%), in which the fissile material is dissolved in the form of fluorides. Fissile material could be ^{233}U, ^{235}U, Pu and/or other TRU, depending on the reactor design [11]. The reactor concept is based on the Molten Salt Breeder Reactor (MSBR) technology developed in the 1965 by the Oak Ridge National Laboratory (ORNL, USA) [12,13]. However, the MSFR design was optimised to overcome the main envisaged MSBR issues, such as unfavourable thermal feedback coefficients, positive void coefficient, required fuel clean-up scheme difficult to achieve and problems specific to the graphite moderator as lifespan, graphite handling and fire risk [14].

The use of a liquid fuel in the MSR concepts brings important technological advantages in comparison to the solid fuel based reactors. E.g., apart from easier on-line reactivity core control, it is a better flexibility of the fuel cycle back-end. In the MSFR, reprocessing of the fuel salt was designed to minimize generation of radiotoxic nuclear waste [10]. For safety assessment and optimisation of the offline MSFR fuel salt reprocessing, which is based on reductive extraction techniques in molten fluoride media [6], thermodynamic and electrochemical properties of the actinides and fission products of interest have to be investigated to determine the separation factors and distribution of these elements within the process. Especially important are data on the activity coefficients, enabling estimation of stability of the compounds present in the reprocessed fuel salt. In this work, an electrochemical technique for evaluation of activity coefficients of compounds dissolved in molten fluoride media was proposed. The selected approach is overcoming an absence of a stable thermodynamic reference electrode for high temperature molten fluoride media. The method was used to experimentally determine ThF_4 activity coefficient in eu-

* Corresponding author.
E-mail address: Pavel.Soucek@ec.europa.eu (P. Souček).

https://doi.org/10.1016/j.electacta.2021.138198

tectic LiF-CaF_2 melt. Up to our knowledge it was done for the first time in this solvent.

A special attention was given to verification of the purity of the input ThF_4 material and the LiF-CaF_2 carrier salt. Similar to other actinide fluorides, ThF_4 is not commercially available in the purity required for electrochemical measurements and it has to be either synthesised or purified. Synthesis of phase pure ThF_4 by fluorination of submicron ThO_2 powder with HF gas has been described in our previous work [15], as well as the established purity control. The X-ray diffraction (XRD) analysis and the melting point determination by differential scanning calorimetry (DSC) did not reveal any detectable impurities in the obtained ThF_4, however, no technique providing direct oxygen quantification was available in this specific case.

Therefore, the electrochemical methods were used for confirmation of the purity and acceptable oxygen content in the synthesised ThF_4 material, based on the review of approaches to determining oxide concentration in molten fluoride salts published by Goh at al. [16] and on the electrochemical studies of oxide ions in molten fluoride media done by Manning and Mamantov [17] and Massot et al. [18]. Cyclic voltammetry (CV) and linear sweep voltammetry (LSV) techniques were selected and proved suitable for this purpose. In the first step, the appropriate electrochemical response of ThF_4 dissolved in a purified LiF-CaF_2 eutectic mixture (80.5–19.5 mol.%) was studied. The studied ThF_4 samples were added into the melt in four different batches in order to step-by-step increase the thorium concentration. Several electrochemical parameters were measured for each thorium content and the results were compared with published data [19–21]. In these experiments, the presence of the dissolved oxygen was analysed and observed before the carrier melt purification. In the second step, a LiF-ThF_4 eutectic salt (78.0–22.0 mol.%) was prepared and characterised by CV and LSV techniques using a gold working electrode to detect the possible oxygen content in ThF_4.

2. Experimental

All experiments and storage and handling of chemicals were carried out in a dry glove box under purified argon atmosphere (O_2/H_2O < 5 ppm) equipped with a hydrogen fluoride gas supply system. A detailed description of the installation has been published in our earlier paper [15]. The electrochemical experiments were carried out in a corrosion-resistant Inconel electrolyser (see Fig. 1 below) inserted in a vertical furnace enabling a maximum working temperature of 1200 °C, built-in to the bottom of the glove box. The electrolyser's lid was equipped with ports for precise guiding and positioning of the electrodes. The electrode holders can be removed fully from the ports, which can be closed gas-tight. Pure HF gas (99.95%, Linde) can be introduced to the electrolyser and used for purification of the liquid melts at high temperatures.

The electrochemical cell consisted of a glassy carbon (GC) crucible containing the measured molten salt and three electrodes. Gold (0.5 mm diameter) and tungsten (1 mm diameter) wires were used for working electrodes, platinum wire (1 mm diameter) served as a quasi-reference electrode as described by Mamantov [22] and reported in the review of Fredrickson [23] and a tungsten wire

(1 mm diameter) as an auxiliary electrode. All the metals were from Alfa-Aesar and had purity 99.99%. The set-up was placed into an alumina crucible electrically insulating the GC crucible from possible shortcuts from the furnace resistance heating system. Inconel electrode holders guided by the ports in the electrolyser's lid were electrically insulated by alumina tubes and further directed by MgO tube sheaths through the electrolyser's heat reflector plates. The electrodes of about 50 mm length were attached to the end of the holders by graphite screw connectors. The active electrode surface was determined after each experiment by measuring the visually distinguishable immersion depth of the electrode in the bath.

A Macor lid was installed on the top of the alumina crucible. It had openings allowing only the electrode holders with the attached electrodes to pass through to prevent contamination of the melt by possible corrosion products from the electrolyser. The temperature was measured using a chromel-alumel thermocouple inserted in an alumina tube sheath and positioned at the level of the studied melt, however not in the direct contact to prevent chemical attack on the sheath. Photos of the set-up are shown in Figs. 1 and 2. All the electrochemical studies were carried out using an Autolab PGSTAT 30 potentiostat controlled with GPES 4.9 software.

The LiF-CaF_2 carrier melt was prepared by mixing the end members (Alfa-Aesar, 99.99 wt.% anhydrous, packed under Ar and opened only inside the dry glove box) in a ratio 80.5–19.5 mol.%, respectively. Around 50 g of the mixture was used for the electrochemical experiments, and the working temperature was 850 °C. The melt was purified according to the procedure described below in Section 3.1. Thorium fluoride synthesised from ThO_2 (JRC Karlsruhe stock material) had a phase purity > 99 wt.% and metal base purity > 99.9 wt.%, based on the gravimetric analysis, XRD, DSC and inductively coupled plasma-mass spectrometry (ICP-MS), as described in detail in [15,24]. ThF_4 was step-wise added to the LiF-CaF_2 carrier salt to form melts with concentration of thorium metal 0.50, 1.01, 1.46 and 1.91 wt.%, i.e., 0.09, 0.18, 0.25 and 0.33 mol.% ThF_4. Finally, an eutectic LiF-ThF_4 melt was prepared by mixing the above mentioned LiF and the synthesised ThF_4 in ratio 78.0–22.0 mol.%, respectively, and it was not purified to be able to evaluate the oxygen content in the ThF_4 initial material.

3. Results and discussion

3.1. Purification of the melt

The carrier LiF-CaF_2 melt was slowly heated up to 850 °C under pure argon gas atmosphere in a glassy carbon crucible, which was thermally treated before the first use by heating to 800 °C for several hours. The melt was characterised by cyclic voltammetry (CV) and linear sweep voltammetry (LSV) measurements using tungsten and gold wires as working electrodes. Although the best purity available materials were used, as described above in Section 2, the LSV on the gold electrode revealed a significant content of oxygen. As illustrated in Fig. 3, the LSV curve showed a sharp increase of current at a potential of +1.5 V vs. Pt quasi-reference electrode. This potential, when related to the melt decomposition potential (not shown on the graph), corresponds to the expected potential of oxygen gas formation [25]. At the same time, the current response was very noisy, indicating evolution of gas bubbles at the electrode surface, which were erratically blocking certain parts of the electro-active surface, leading to changes of the current value and causing the noisy signal. Although the method was not calibrated and the absolute value of the oxygen concentration could not be evaluated, the measurement clearly indicated oxygen content and the melt had to be purified.

In order to remove the dissolved oxide ions, the LiF-CaF_2 melt was purified by fluorination by HF gas, which was bubbled directly into the melt using a tube made from pure nickel metal (99.9 wt.%) for 120 min at 850 °C with a flow rate of 6 cm^3/min. All parts from alumina were removed from the set-up to prevent their reaction with HF gas and possible contamination of the melt by the reaction products. The glassy carbon crucible with the melt was placed on a small Macor plate to ensure electric insulation from the fur-

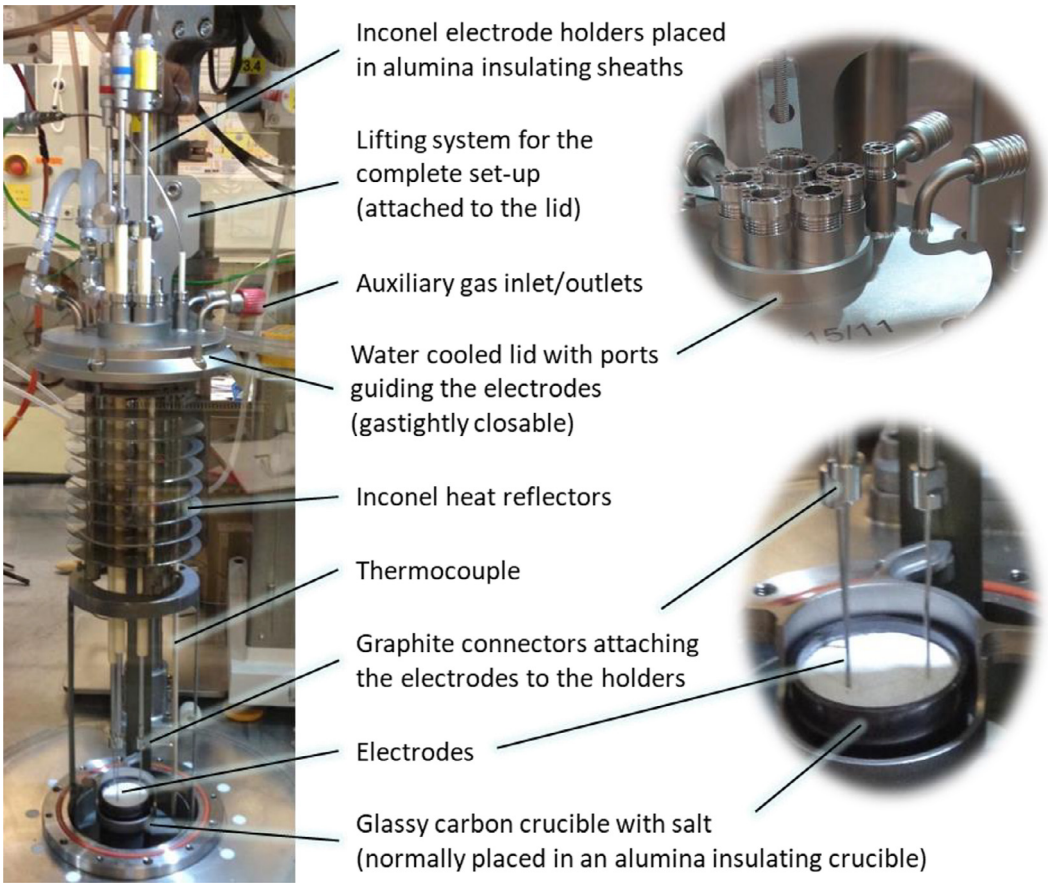

Fig. 1. Photo of the electrolyser with description of the most important parts. The insulating alumina crucible with the lid and the electrode holders guiding MgO tubes are not shown.

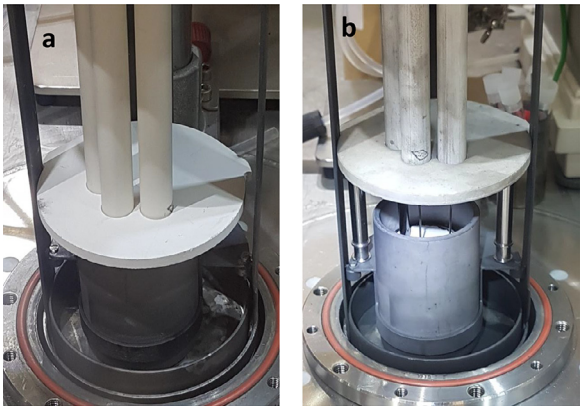

Fig. 2. Photo of the electrochemical cell consisting of insulating alumina crucible with glassy carbon crucible inside (not visible), a Macor lid and three electrode set-up with MgO tube sheaths for guidance of the electrode holders. Detail of the set-up with the lid in closed (a) and opened (b) position.

nace. HF gas is expected to react with the dissolved oxygen ions according to the reaction:

$$O^{2-}(sln) + 2HF(g) \rightarrow H_2O(g)\uparrow + 2F^{-}(sln). \quad (1)$$

After the fluorination, the dissolved excess of HF gas was removed from the melt by bubbling of pure argon gas. The efficiency of the HF gas treatment was proven by another LSV measurement on the gold electrode. As shown in Fig. 3, the previously observed current increase corresponding to the oxygen gas formation was no longer detected and the oxide ions concentration was assumed negligible. The anodic reaction indicated by a sharp increase of current at a potential of 2.50 V vs. Pt was oxidation of the gold electrode $Au(s) + e^{-} \rightarrow Au^{+}(sln)$. In addition, the CV on tungsten electrode revealed an excellent purity of the melt concerning dissolved metallic ions both before and after the purification. As shown on the CV curve in Fig. 3 (an insert in the LSV graph), there was no detectable current response of any dissolved metallic impurities. The electrode reactions defining the oxidation and reduction potential limits observed on the CV are described in Section 3.3 below.

3.2. Effect of oxygen dissolved in a LiF-CaF_2 melt

Purification of the carrier LiF-CaF_2 melt from the dissolved oxygen was necessary to avoid formation of partly soluble thorium oxyfluoride $ThOF_2$ [26] and/or precipitation of thorium in the form of ThO_2 after addition of ThF_4 to this melt. If thorium would precipitate as insoluble oxide, the electrochemical response of the remaining dissolved thorium would not be influenced, but the concentration of thorium ions in the melt would not correspond to the addition of ThF_4.

However, an important splitting of Th(IV)/Th electrochemical peaks was observed during our initial experiments using ThF_4 dissolved in a non-purified LiF-CaF_2 melt containing oxygen. As shown in Fig. 4, it was not possible to evaluate correctly the obtained thorium cyclic voltammogram and square-wave voltammogram (SWV) due to the Th(IV)/Th redox peak doubling. Although this hypothesis could not be proved conclusively, it was likely caused by the presence of thorium in the melt in a form of both

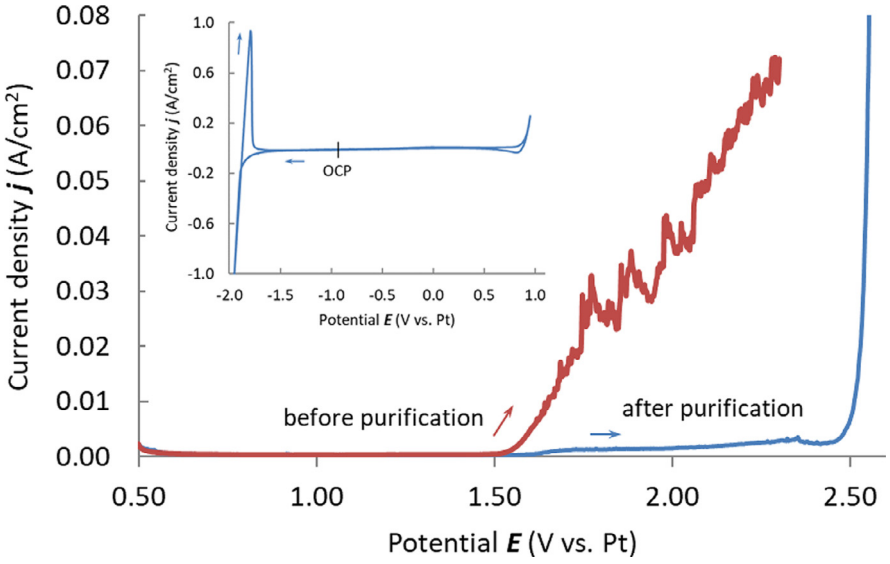

Fig. 3. Linear sweep voltammetry of LiF-CaF_2 eutectic melt before (thick line) and after (thin line) purification by HF gas, working electrode: Au wire (S = 0.08 cm^2), counter electrode: glassy carbon rod, quasi-reference electrode: Pt wire, scan rate: 10 mV/s, temperature: 850 °C. Insert in the graph: Cyclic voltammetry in the cathodic domain of the same melt after purification, working electrode: W wire (S = 0.16 cm^2), counter electrode: glassy carbon rod, quasi-reference electrode: Pt wire, scan rate: 100 mV/s, temperature: 850 °C.

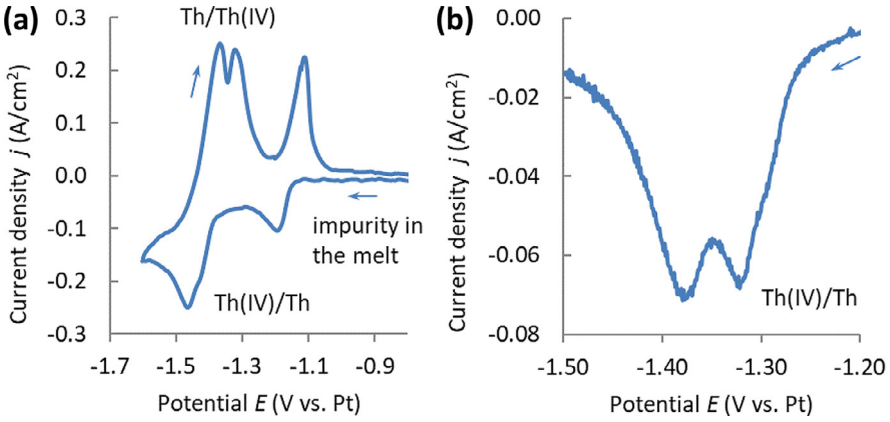

Fig. 4. Cyclic voltammogram (a) and square-wave voltammogram (b) of ThF_4 in non-purified LiF-CaF_2 eutectic melt containing some dissolved oxygen, working electrode: W wire (S = 0.16 cm^2), counter electrode: glassy carbon rod, quasi-reference electrode: Pt wire, temperature: 850 °C. CV scan rate: 100 mV/s, SWV frequency 9 Hz, amplitude $1 \cdot 10^{-3}$ V.

fluoride and oxyfluoride, the latter one formed by a chemical reaction of the added ThF_4 with the oxide ions present in the carrier melt. Except the oxygen, the used melt also contained an unidentified, likely metallic impurity, evidenced by a peak with a characteristic shape for a soluble-insoluble electrochemical system at a potential of −1.15 V vs. Pt, as visible on the CV curve in the Fig. 4 (left). However, the electrochemical response did not indicate formation of any alloys between this impurity and Th, as no anodic peaks or waves were observed at potentials more positive than Th(IV)/Th red-ox potential. At the same time, the observed CV peak splitting could be characteristic for a presence of fluoride and oxyfluoride, as described previously by several authors in the electrochemical studies on niobium fluoride and oxyfluoride complexes in alkali fluorides and chlorides based molten salt media [27–31]. In addition, it was proven that the used ThF_4 did not contain the detected impurity, as after addition of more ThF_4, only the peak corresponding to the Th(IV)/Th red-ox system increased. Therefore, it was concluded that the splitting was not caused by the presence of the metallic impurity, but only by the effect of oxide ions content in the non-purified melt.

3.3. *Electrochemical behaviour of ThF_4 in purified LiF-CaF_2*

Cyclic voltammetry was carried out on tungsten in the purified LiF-CaF_2 eutectic melt. The cathodic limit of the electrochemical window corresponded to the decomposition of the melt, i.e., reduction of the least stable cation of the solvent Li(I) to Li metal, as shown in [32] and further discussed below in Section 3.5, and the anodic limit was due to the oxidation of the working electrode material. Fig. 5 shows the cyclic voltammogram of the blank LiF-CaF_2 melt using a W working electrode, clearly demonstrating both potential limits.

Thorium was step-wise introduced in the LiF-CaF_2 carrier salt in a form of ThF_4 powder and the melt was electrochemically characterised after each addition. Concentration of thorium in the formed melts was 0.50, 1.02, 1.46 and 1.91 wt.%. Sharp cathodic and anodic peaks at a potential of −1.64 V vs. Pt were detected in the cyclic voltammograms after the addition of ThF_4, as shown in Fig. 5 for the case of a melt containing 1.02 wt.% Th. The shape of the signal was characteristic of a solid-soluble redox system and the value of the peak potential related to the melt decomposition was in a good

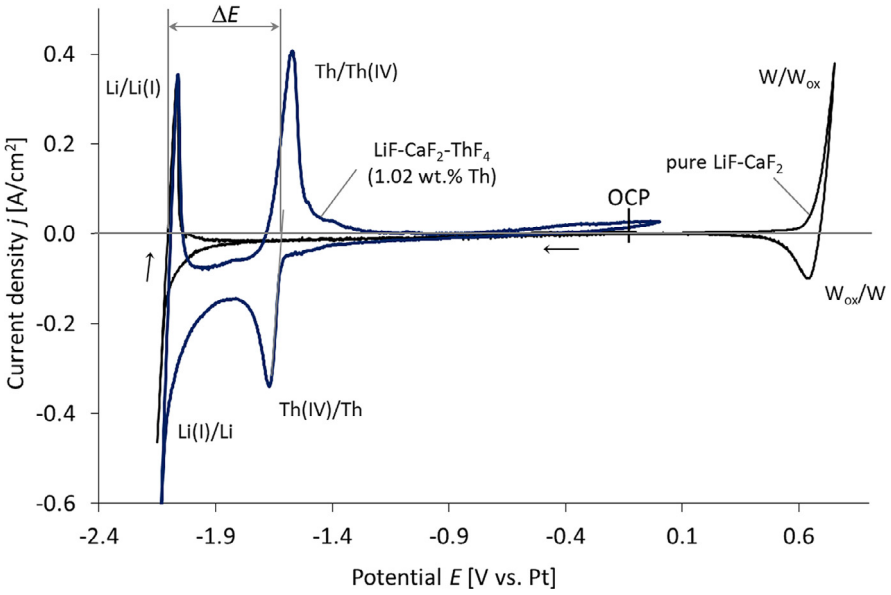

Fig. 5. Cyclic voltammetry of pure LiF-CaF_2 eutectic melt and LiF-CaF_2-ThF_4 (1.02 wt.% Th) melt on W working electrode (S = 0.31 cm^2), W counter electrode and Pt quasi-reference electrode at a temperature of 850 °C and scan rate 100 mV/s. The ΔE graphical evaluation is described below in the Section 3.5 and in Fig. 9.

agreement with the potential of Th(IV)/Th redox system in the LiF-CaF_2 melt, as published in [19–21]. Therefore, the peaks were attributed to the reduction of Th(IV) to Th metal and its re-oxidation according to Eq. (2):

$$\mathrm{Th(IV)(sln)} + 4e^- \leftrightarrow \mathrm{Th(s)} \quad (2)$$

In both Th(IV)/Th and Li(I)/Li redox systems, a slight negative current slope was observed prior reduction to metals at the beginning of the cathodic peaks, as well as low intensity anodic current waves after the dissolution of the metals from the working electrode surface during the back scans. The phenomenon indicates possible formation and re-oxidation of thin surface alloys of the deposited metals with material of the working electrode, with possibly presented traces of dissolved impurities and/or with each other. This effect can be enhanced by high working temperature and presence of very reactive actinide and lithium metals. Slight increase of the anodic current at a potential of about −0.4 V vs. Pt quasi-reference electrode can be also explained by an overpotential re-oxidation of these surface alloys and it can be assumed as not significant for evaluation of the studied system. An effect of oxide ions dissolved in the melt can be excluded, as no other evidence of the oxygen presence was observed, such as splitting of Th(IV) reduction and oxidation peaks (see discussion in Section 3.2 and Fig. 4 above).

The Th(IV) reduction peak current density j_p increased linearly with the thorium concentration increase, as shown in Fig. 6. It indirectly confirmed the assignment of the observed system to the Th(IV)/Th red-ox couple and it also indicated no side reaction of the dissolved Th with any possibly present impurity, which would not be detected by the electrochemical measurements. A slight shift of the Th(IV)/Th cathodic peak potential E_{pc} towards negative values was observed, showing 0.03 V difference between the lowest and highest Th concentration.

Cyclic voltammetry of the Th(IV)/Th red-ox system was measured using different scan rates in a range from 50 to 500 mV·s^{-1} for the melt containing 1.02 wt.% Th. The values of the Th(IV)/Th cathodic peak potential E_p were found constant with the scanning potential rate variation except one experimental point from eight measurements, which was exceeding the constant value for +0.02 V. The point was likely affected by a short instability of the

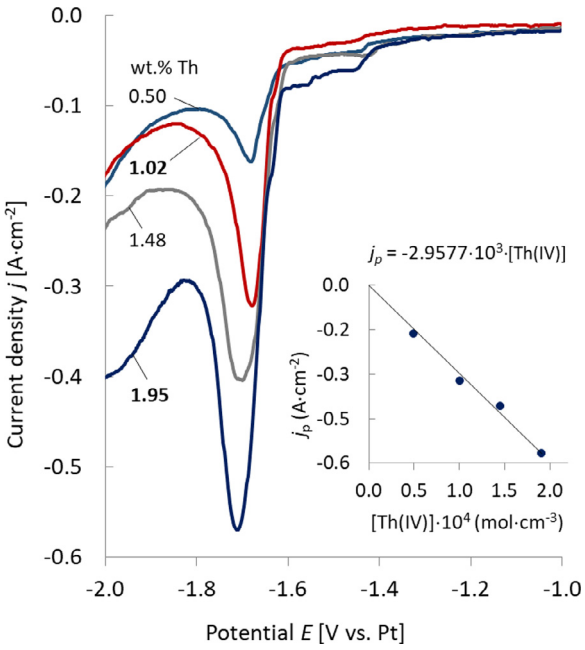

Fig. 6. Th(IV)/Th reduction peaks measured by cyclic voltammetry in LiF-CaF_2-ThF_4 melts containing 0.50, 1.02, 1.48 and 1.95 wt.% of Th, scan rate 100 mV/s. The insert shows the linear dependency of the Th(IV) reduction peak current density j_p on the Th(IV) concentration recalculated to mol·cm^{-3} units for the purpose of evaluation the Th(IV) diffusion coefficient described below. All voltammograms were measured using W working electrode (S = 0.31 cm^2), W counter electrode and Pt quasi-reference electrode at a temperature of 850 °C. (For interpretation of the references to colour in this figure legend, the reader is referred to the web version of this article.)

quasi-reference electrode and it was not taken into account. The observed independency of the peak potential on the scan rate characterizes a reversible redox system (see graph in Fig. 7, secondary axis). However, for a reversible system, the above-shown shift of the Th(IV)/Th cathodic peak potential should be towards positive values. In the present case, the determination of the peak potentials measured long time after each other can be significantly affected by a potential shift of the used Pt quasi-reference electrode,

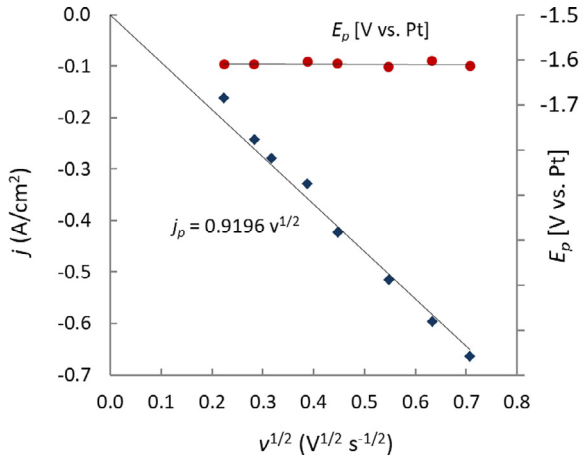

Fig. 7. Variation of the Th(IV)/Th peak current density j_p (primary axis) and cathodic peak potential E_p (secondary axis) with the scan rate $v^{1/2}$ obtained in the melt LiF-CaF_2-ThF_4 (1.02 wt.% Th).

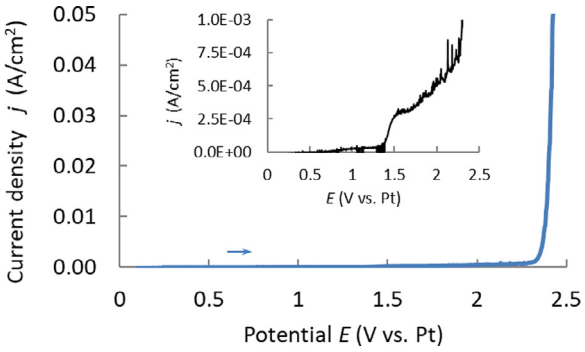

Fig. 8. Linear sweep voltammetry of LiF-ThF_4 eutectic melt on Au working electrode (S = 0.16 cm^2), counter electrode W, quasi-reference electrode Pt, temperature 850 °C, scan rate 100 mV/s (CV) and 10 mV/s (LSV). Only the anodic domain is shown to better illustrate the possible oxygen electrochemical response. The insert shows a zoom of the low current intensity region.

which can be caused by slightly increasing concentration of oxygen ions dissolved in the measured, highly hygroscopic and oxygen sensitive fluoride melt. It can result in a shift of potentials measured over a long period of time to negative values. This effect could have possibly overruled the expected positive potential shift and turn it to a slightly negative shift of 20 mV, as observed. Thus, the obtained results indicate that the system is electrochemically reversible, however, it was not conclusively proven.

The reduction peak current density j_p was increasing with the scan rate and it was following a linear dependency on the square root of the scanning potential rate $v^{1/2}$ for all the concentrations (see graph in Fig. 7, primary axis). It indicates that the observed Th electrochemical reduction process is controlled by the diffusion of Th(IV) ions in the solution.

The linear regression calculated with the experimental variation of j_p vs. $v^{1/2}$ yielded a straight line passing through the origin, which is expected for an electrochemical process controlled by diffusion [33]. Assuming electrochemical reversibility of the Th(IV)/Th reduction process, although not conclusively justified, this analysis enabled a determination of the diffusion coefficient of Th(IV) in the LiF-CaF_2 melt using the obtained value $j_p = 0.9196 \cdot v^{1/2}$ and the Eq. (3) established by Berzins and Delahay [34] for a reversible, soluble/insoluble system:

$$i_p = 0.61nFS[Th(IV)]_{sln}\left(\frac{nFD_{Th(IV)}v}{RT}\right)^{1/2} \quad (3)$$

where i_p is the measured peak current, S is the working electrode surface area (cm^2), $[Th(IV)]_{sln}$ is the concentration of Th(IV) in the molten salt (mol.cm^{-3}), v is the scan rate (V.s^{-1}) and other variables were defined above. The obtained value of the Th(IV) diffusion coefficient at a temperature of 850 °C and a concentration of 1.02 wt.% Th = $1.01 \cdot 10^{-4}$ mol.cm^{-3} was $D_{Th(IV)} = 3.62 \cdot 10^{-5}$ cm$^2 \cdot s^{-1}$.

In addition, the Th(IV) diffusion coefficient was calculated using the dependency of the peak current density on the Th(IV) concentration in the melt (see insert in Fig. 6 left) for a selected constant scan rate 100 mV$\cdot s^{-1}$. The linear regression yielded a value of $j_p = -2.9577 \cdot 10^3 \cdot [Th(IV)]$ and a value of Th(IV) diffusion coefficient $D_{Th(IV)} = 3.82.10^{-5}$ cm$^2.s^{-1}$. The agreement reached between these two values indicates a sufficient accuracy of the experimental measurements. In addition, the order of magnitude of the evaluated diffusion coefficient is similar to the data published for thorium [20] and uranium [35,36] in molten fluoride salt media at temperatures higher than 800 °C.

3.4. Electrochemical purity of a LiF-ThF_4 melt

The above-described characterisation of ThF_4 in a LiF-CaF_2 melt showed an excellent electrochemical purity of all used chemicals, however, it did not conclusively quantify the possible oxygen content in the synthesized ThF_4. A small concentration of oxygen in ThF_4 would likely not be observed in the measurements, since its content in the melt would be very low. Therefore, LiF-ThF_4 (78.0–22.0 mol.%) eutectic melt was prepared and characterized by cyclic voltammetry and linear sweep voltammetry on a gold electrode. To be able to measure the possible oxygen content, the melt was not purified before the measurement. Both techniques showed only traces of the dissolved oxygen ions in the melt. The maximum detected current density at the potential corresponding to the oxygen formation before the sharp current increase due to oxidation of the Au electrode was $7.5 \cdot 10^{-4}$ A$\cdot$cm^{-2}, as shown in Fig. 8. Since the ThF_4 content in the LiF-ThF_4 melt was high (78 wt.%), the results indicated that the synthesized ThF_4 does not contain any important amount of oxygen. In addition, this experiment showed that the used commercially available LiF is almost free from oxygen impurities and the oxygen content detected in the LiF-CaF_2 melt, as discussed in detail above in Section 3.1, consequently originated from the used CaF_2.

3.5. Activity coefficient of ThF_4 in LiF-CaF_2 eutectic melt

The thermodynamic activity coefficient is related to the stability of a component in a solution. It is a measure for the deviation from ideal behaviour (if any) of the components of the - in our case - liquid mixture. The lower the activity coefficient, the higher the affinity of the species to the solvent, and the more stable the species is in the solvent. A technique to determine the activity coefficient in molten fluoride salt by electrochemical techniques is proposed and described in this section.

The electrochemical stability of a chemical species composed of a metal M^{y+} and a halide X^- ions, MX_y, in a selected standard state dissolved in a molten halide solvent is characterized by a standard (thermodynamic) potential $E^0_{MX_y/M}$. The experimentally accessible potential $E_{MX_y/M}$ of the species MX_y in a real, non-standard state is lower than the standard electrode potential due to the interaction of the species with the solvent, i.e., its solvation. The difference between $E^0_{MX_y/M}$ and $E_{MX_y/M}$ depends on an activity of the species $a(MX_y)$ and thus also on the activity coefficient $\gamma(MX_y)$ according to the Eq. (4)

$$a(MX_y) = x(MX_y)\ \gamma(MX_y), \quad (4)$$

Table 1
Results of calculation of the standard potentials using JRCMSD database and data for pure compounds at a reaction temperature of 850 °C.

Redox reaction	ΔG (J·mol^{-1})	E^0 (V/F_2/F^-)
$ThF_4 \leftrightarrow Th + 2F_2(g)$	1,756,877	−4.55
$LiF \leftrightarrow Li + 0.5F_2(g)$	508,677	−5.27
$CaF_2 \leftrightarrow Ca + F_2(g)$	1,036,862	−5.37

where $x(MX_y)$ is a concentration of the species MX_y expressed as its molar fraction.

In chloride media (X = Cl), the activity coefficient can be obtained from the measured equilibrium potential and the standard potential calculated from available data, as both can be related to the same thermodynamic reference Cl_2/Cl^-, as done e.g. for $ThCl_4$ by Cassayre et al. [37] and by Delpech [33]. In contrast, so far the activity coefficient could not be determined experimentally in a similar way in high-temperature fluoride media due to the lack of a stable thermodynamic reference electrode that can be used in experiments.

The electrochemical reaction of the studied Th(IV)/Th redox system and the associated Nernst relation can be expressed by Eqs. (5) and (6):

$$ThF_4 + 4e^- \rightarrow \ Th_{(s)} + 4F^- \tag{5}$$

$$E_{ThF_4/Th} = E^0_{ThF_4/Th} + \frac{RT}{4F} \ln \frac{a(ThF_4)}{a(F^-)^4 \ a(Th)}, \tag{6}$$

in which $E_{ThF4/Th}$ is an equilibrium potential of the redox system Th(IV)/Th, which can be experimentally measured in the salt, $E^0{}_{ThF4/Th}$ is the standard potential of the redox system Th(IV)/Th calculated using thermodynamic data, a(i) is the activity of the specie i in the solvent and other variables are explained above in the text. Eq. (6) cannot be directly used to calculate the activity of ThF_4 (and thus the activity coefficient according to eq. (3)) due to two reasons: (i) the experimentally obtained ThF_4/Th equilibrium potential $E_{ThF_4/Th}$ does not refer the standard thermodynamic potential $E^0_{ThF_4/Th}$ and (ii) the activity of fluoride ions $a(F^-)$ in LiF-CaF_2 melt is unknown. Nevertheless, the cathodic limit of the used solvent can be used as a reference potential, as published by Gibilaro for determination of thermodynamic properties in high temperature molten salt media showed on an example of CeF_3 in eutectic LiF-CaF_2 [38] and by Delpech for evaluation of the activity coefficient of ZrF_4 in LiF-ThF_4 molten salt [39].

In the studied case, the cathodic limit is corresponding to Li(I)/Li redox system, as discussed above in Section 3.3 and below Table 1). The electrochemical reaction of this system and the associated Nernst relation can be expressed as Eqs. (7) and ((8):

$$LiF + e^- \rightarrow Li_{(s)} + F^- \tag{7}$$

$$E_{LiF/Li} = E^0_{LiF/Li} + \frac{RT}{F} \ln \frac{a(LiF)}{a(F^-) \ a(Li)} \tag{8}$$

The evaluation of ThF_4 activity coefficient was based on an experimental measurement of a difference between Th(IV)/Th and Li(I)/Li equilibrium potentials and comparing this value with calculated difference between Th(IV)/Th and Li(I)/Li standard potentials, as described below.

The LiF/Li electrode reaction (7) can be rewritten in a form to involve 4 electrons exchange, i.e., for the reduction of 4 mol of LiF to comply with the overall studied reaction ThF_4 + 4Li ↔ 4LiF + Th, with the correspondingly modified Nernst relation (8) yielding Eq. (9):

$$E_{LiF/Li} = E^0_{LiF/Li} + \frac{RT}{4F} \ln \frac{a(LiF)^4}{a(F^-)^4 \ a(Li)^4} \tag{9}$$

The potential difference $\Delta E = \ E_{LiF/Li} - E_{ThF_4/Th}$ can be then expressed by deducing the relation (6) from relation (9) yielding Eq. (10):

$$\Delta E = \ E_{LiF/Li} - E_{ThF_4/Th} = E^0_{LiF/Li} - \ E^0_{ThF_4/Th} + \frac{RT}{4F} \ \ln \frac{a(LiF)^4}{a(ThF_4)} \tag{10}$$

The activities of thorium and lithium metals $a(Th)$ and $a(Li)$ in Eq. (6) and (9) are equal to 1 and the unknown activities of fluoride ions $a(F^-)$ mathematically cancel out each other by the deduction of the equations.

The difference of equilibrium potentials ΔE was experimentally measured using cyclic voltammetry, while the standard potentials $E^0_{LiF/Li}$ and $E^0_{(ThF_4/Th)}$ were calculated with the FactSage software using a Joint Research Centre Molten Salt Database (JRCMSD, developed at JRC Karlsruhe), where the data for pure compounds were adopted from [[40], [41]]. The values of the standard potentials E^0 were derived from the calculation of the Gibbs enthalpies ΔG^0 of the corresponding chemical reactions at the reaction temperature of 850 °C using the relation (11):

$$E^0 \ = -\Delta G^0/nF \tag{11}$$

The obtained values of the standard potentials, the corresponding chemical reactions and the values of the Gibbs enthalpies are given in Table 1 for both redox systems of interest ThF_4/Th and LiF/Li, together with the calculated values for the system CaF_2/Ca in order to additionally prove that the melt decomposition limit is corresponding to the less stable LiF/Li system.

The activity $a(LiF)$ in the used LiF-CaF_2 eutectic solvent was also calculated using the FactSage software and the JRCMSD database to be 0.798, which agrees with the published value calculated for temperature 876 °C in [42]. The activity value is very close to the mole fraction of LiF in the mixture (0.795), which indicates that the excess Gibbs energy for the solution formation is small and the activity coefficient of LiF at the given conditions is almost equal to unity.

The ΔE value of −0.46 V was experimentally obtained from the cyclic voltammetry measurements described above in Section 3.3 as a difference between the equilibrium potentials Th(IV)/Th and Li(I)/Li. These potentials were graphically evaluated from the cathodic peaks of the measured cyclic voltammograms, not using the initial current slope likely indicating formation of surface alloys prior the pure metals deposition, as discussed above in Section 3.3. The negative slope of the peaks corresponding to the deposition of pure metals, i.e., the part where the metal deposited on the electrode surface is in equilibrium with the specie dissolved in the bulk of the melt, was extrapolated to zero current and the obtained potential value was estimated as equilibrium potential. The graphical evaluation of both Th(IV)/Th and Li(I)/Li equilibrium potentials is shown in Fig. 9.

Using all the above described data, the activity of ThF_4 was calculated from Eq. (10) to be $a(ThF_4) = 8.74 \cdot 10^{-6}$ and with the concentration of dissolved ThF_4 as 0.18 mol.%, the activity coefficient of ThF_4 was determined to be $\gamma(ThF_4) = 4.85 \cdot 10^{-3}$ using Eq. (4). Table 2 shows a comparison of this value was with the data for the ThF_4 activity coefficients obtained during our previous work [43,44] for different molten fluoride salt. The used reference state is the pure compounds, expressed as mole fraction for solid and liquid compounds and partial pressure for gaseous compounds.

The ThF_4 activity coefficient measured in our work in the LiF-CaF_2 melt is about 4 orders of magnitude higher than in the LiF-NaF-KF eutectic melt. The reason is the different activity of free fluoride ions F^- in these melts, which affects the affinity of ThF_4 towards the solvents. As discussed in [45], alkali fluorides molten salts are almost fully dissociated and the F^- activity in these solvents can be approximated as 1. The F^- concentration is relatively

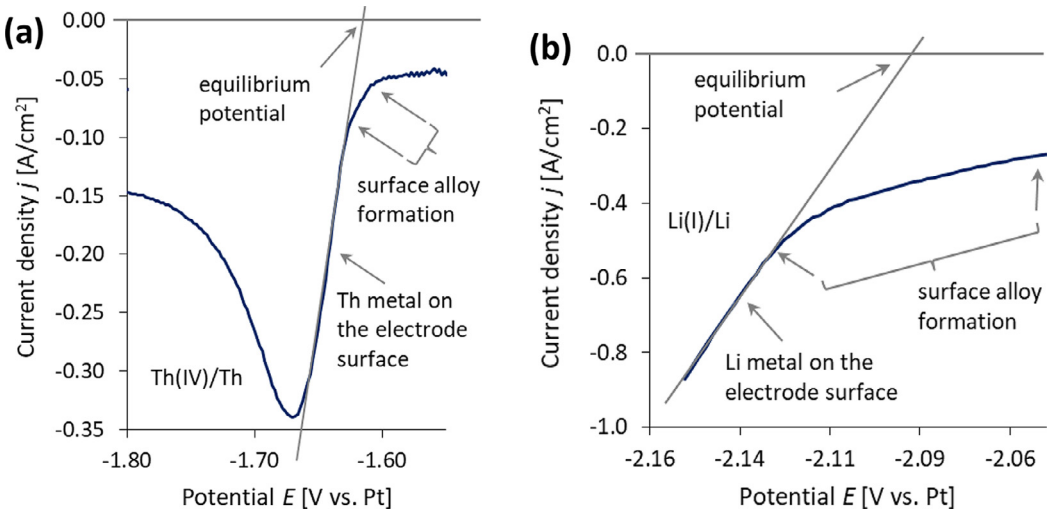

Fig. 9. Graphical evaluation of Th(IV)/Th (a) and Li(I)/Li (b) equilibrium potentials from cyclic voltammetry of LiF-CaF_2-ThF_4 (1.02 wt.% Th) melt on W working electrode ($S = 0.31$ cm^2), W counter electrode and Pt quasi-reference electrode at a temperature of 850 °C and scan rate 100 mV/s.

Table 2
Comparison of activity coefficients of ThF_4 in different molten salts using pure compounds as reference state.

Solvent	LiF-CaF_2 (this work) (79.5–20.5 mol.%)	LiF-NaF-KF [44] (46.5–11.5–42.0 mol.%)	LiF-ThF_4 [43] (80–20 mol.%)	LiF-ThF_4 [44] (76–24 mol.%)
Temperature	850 °C	600 °C	600 °C	600 °C
log γ (ThF_4)	−2.31	−6.54	−2.62	−1.80
x(ThF_4) mol.%	0.18	1.07	20.0	24.0

high in these melts, resulting in strong bonding and strong solvation of thorium. As shown in the following paragraph, CaF_2 has higher affinity to F^- ions and from a certain content in a mixture, CaF_2 decreases the F^- ions concentration and the thorium solvation. Therefore, ThF_4 has higher activity coefficient in the LiF-CaF_2 melt than in the LiF-NaF-KF melt.

Numakura et al. [46] studied ThF_4-LiF-CaF_2 melts with fixed content of ThF_4 (25 mol.%) and with increasing concentration of CaF_2 (up to 40 mol.%) by EXAFS measurements. They found an average coordination number of thorium molecular complexes $[ThF_n]^{4-n}$ to be $n = 7.1 - 7.3$ at $T = 1073$ K, dependant on the CaF_2 concentration. They observed disordering of the local structure around Th^{4+} up to the CaF_2 molar fraction 0.17, while above that concentration, the Th^{4+} local structure stabilised as a result of the decrease of the number density of free fluorine ions F^- in the melts. From this observation, they concluded that CaF_2 acts as F^- donor for CaF_2 molar fraction < 0.17, whereas F^- in the mixture is diluted above that concentration.

It can be assumed that the free fluorine concentration in the LiF-ThF_4 eutectic melt is in a comparable range as in the LiF-CaF_2 eutectic melt. Both media are containing higher valence cations with high affinity towards free fluorine ions and in addition, the ThF_4 activity coefficient in the LiF-CaF_2 melt determined in this work is similar to the value of ThF_4 activity coefficients published for LiF-ThF_4 melts. If the above assumption would be correct, the thorium molecular complexes in the measured LiF-CaF_2-ThF_4 melt would be likely similar as in the LiF-ThF_4 melts. The coordination number found in the above-mentioned work by Numakura et al. [46] in the pure LiF-ThF_4 melt was $n = 7.0$. In comparison, Bessada et al. [47] investigated the LiF-ThF_4 (5–50 mol.% ThF_4) systems by EXAFS experiments and molecular dynamics simulations and they reported that the main observed anionic species in the melt had coordination numbers 7, 8 and 9, with the predominantly present complex $[ThF_8]^{4-}$ for all studied ThF_4 compositions at temperatures 973–1223 K.

Summary and conclusions

The results of the work have shown that electrochemical characterization is an advantageous method to prove the purity of fluoride melts, especially with regard to oxygen content. Cyclic voltammetry and linear sweep voltammetry techniques using a gold working electrode are supplementary methods to reveal the presence of oxygen in the melts. These techniques have been applied to characterize non-purified and purified LiF-CaF_2 eutectic melts and a ThF_4 previously synthesized from ThO_2. The electrochemical response has shown the expected presence of oxygen in the non-purified LiF-CaF_2 melt, while in the cases of purified melt and of ThF_4 dissolved in a pure LiF forming an eutectic LiF-ThF_4 melt, no signal related to oxygen content has been observed. Although the method has not been calibrated to quantify the oxygen content, it has proved sufficient to demonstrate the purity of the fluorides for electrochemical studies. The consecutive measurements have shown the expected responses, not affected by any chemical reactions with oxygen.

In addition to the confirmation of the absence of oxygen impurity, the cyclic voltammetry technique has been used to show the ThF_4 purity from metallic impurities soluble in the studied LiF-CaF_2 molten salt solvent. Combination of all results has proven the usability of the ThF_4 material for the study on its thermodynamic properties.

The most important difficulties for the experimental measurement of thermodynamic and electrochemical properties in high temperature molten fluoride media are the absence of a stable thermodynamic reference electrode and the unknown value of activity of free fluorine ions in many molten fluoride solvents. The presented method for determination of activity coefficient is overcoming both problems. It is based on measurements of difference between the electrode potentials of the studied compound and the least stable carrier melt constituent (melt decomposition potential). The activity coefficient of the compound can be calculated

from this experimentally obtained potential difference, assuming that the standard electrode potentials of the compound and the least stable solvent constituent are known or can be calculated, as well as the activity of the least stable solvent constituent. This activity is often assumed to be equal to its molar faction in the solvent, but that is not correct in some cases, e.g., LiF-ThF_4 or LiCl-KCl based molten salt media. The relative potential measurement does not require any stable reference electrode. In addition, this approach is using the fact that even if the free fluorine activity is unknown in the measured melt, it is a constant value for each solvent and when using a potential difference, this value is excluded from the calculation and thus does not have to be known.

The above-described approach has been used in this work to evaluate the activity coefficient of ThF_4 in LiF-CaF_2 eutectic melt by measuring a difference between the Th(IV)/Th electrode potential and the melt decomposition potential, corresponding to the Li(I)/Li red-ox couple. The ThF_4 activity coefficient has been determined using the calculated activity of LiF in the LiF-CaF_2 solvent and the LiF/Li and ThF_4/Th standard potentials. The obtained value is in the expected order of magnitude and comparable to the published data on activity coefficients of actinides in molten fluoride media.

Therefore, we conclude that the presented method can be used for experimental determination and comparison of activities and activity coefficients of different solutes in any fluoride melt, for which the above-mentioned thermodynamic data required for the calculation, are available.

Declaration of Competing Interest

None.

Acknowledgement

The authors wish to thank colleagues from JRC-Karlsruhe and CNRS-IPNO for help and valuable discussions. This work was carried out with the European Commission financial support in the Horizon 2020 framework program, under the collaborative projects “SAMOFAR”, grant agreement number 661891 - SAMOFAR: A Paradigm Shift in Nuclear Reactor Safety with the Molten Salt Fast Reactor and “SAMOSAFER”, grant agreement number 847527 - SAMOSAFER: Severe Accident Modelling and Safety Assessment for Fluid-fuel Energy Reactors.

References

[1] M. Allibert, M. Aufiero, M. Brovchenko, S. Delpech, V. Ghetta, D. Heuer, A. Laureau, E. Merle-Lucotte, 7 - Molten salt fast reactors, in: I.L. Pioro (Ed.), Handbook of Generation IV Nuclear Reactors, Woodhead Publishing, 2016, pp. 157–188.
[2] M. Brovchenko, D. Heuer, E. Merle-Lucotte, M. Allibert, V. Ghetta, A. Laureau, P. Rubiolo, Design-related studies for the preliminary safety assessment of the molten salt fast reactor, Nucl. Sci. Eng. 175 (3) (2013) 329–339.
[3] X. Doligez, D. Heuer, E. Merle-Lucotte, M. Allibert, V. Ghetta, Coupled study of the Molten Salt Fast Reactor core physics and its associated reprocessing unit, Ann. Nucl. Energy 64 (2014) 430–440.
[4] G. Durán-Klie, D. Rodrigues, S. Delpech, Dynamic reference electrode development for redox potential measurements in fluoride molten salt at high temperature, Electrochim. Acta 195 (2016) 19–26.
[5] E. Merle-Lucotte, L. Mathieu, D. Heuer, V. Ghetta, R. Brissot, C. Le Brun, E. Liatard, Influence of the processing and salt composition on the thorium molten salt reactor, Nucl. Technol. 163 (2008) 358–365.
[6] D. Rodrigues, G. Durán-Klie, S. Delpech, Pyrochemical reprocessing of molten salt fast reactor fuel: focus on the reductive extraction step, Nukleonika 60 (4) (2015) 907–914.
[7] SAMOFAR: A paradigm shift in reactor safety with the molten salt fast reactor, European Commission, Horizon 2020 project factsheet, available online: https://cordis.europa.eu/project/rcn/196909/factsheet/en (Accessed April 2020).
[8] in: J.L. Kloosterman, 20 - safety assessment of the molten salt fast reactor (SAMOFAR), in: T.J. Dolan (Ed.), Molten Salt Reactors and Thorium Energy, Woodhead Publishing, 2017, pp. 565–570.
[9] SAMOSAFER: Severe accident modeling and safety assessment for fluid-fuel energy reactors, European Commission, Horizon 2020 project factsheet, available online: https://cordis.europa.eu/project/id/847527 (Accessed April 2020).
[10] S. Delpech, E. Merle-Lucotte, D. Heuer, M. Allibert, V. Ghetta, C. Le-Brun, X. Doligez, G. Picard, Reactor physic and reprocessing scheme for innovative molten salt reactor system, J. Fluor. Chem. 130 (1) (2009) 11–17.
[11] C. Fiorina, M. Aufiero, A. Cammi, F. Franceschini, J. Krepel, L. Luzzi, K. Mikityuk, M.E. Ricotti, Investigation of the MSFR core physics and fuel cycle characteristics, Prog. Nucl. Energy 68 (2013) 153–168.
[12] H.G. MacPherson, The molten salt reactor adventure, Nucl. Sci. Eng. 90 (1985) 374–380.
[13] M.E. Whatley, L.E. McNeese, W.L. Carter, L.M. Ferris, E.L. Nicholson, Engineering development of the MSBR fuel recycle, Nucl. Appl. Technol. 8 (2) (1970) 170–178.
[14] J. Serp, M. Alibert, O. Beneš, S. Delpech, O. Feynberg, V. Ghetta, D. Heuer, D. Holcomb, V. Ignatiev, J.L. Kloosterman, L. Luzzi, E. Merle-Lucotte, J. Uhlíř, R. Yoshioka, D. Zhimin, The molten salt reactor (MSR) in generation IV: overview and perspectives, Prog. Nucl. Energy 77 (2014) 308–319.
[15] P. Souček, O. Beneš, B. Claux, E. Capelli, M. Ougier, V. Tyrpekl, J.F. Vigier, R.J.M. Konings, Synthesis of UF4 and ThF4 by HF gas fluorination and re-determination of the UF4 melting point, J. Fluor. Chem. 200 (2017) 33–40.
[16] B. Goh, F. Carotti, R.O. Scarlat, A review of electrochemical and non-electrochemical approaches to determining oxide concentration in molten fluoride salts, ECS Trans 85 (13) (2018) 1459–1471.
[17] D.L. Manning, G. Mamantov, Electrochemical studies of oxide ions and related species in molten fluorides, J. Electrochem. Soc. 124 (4) (1977) 480–483.
[18] L. Massot, L. Cassayre, P. Chamelot, P. Taxil, On the use of electrochemical techniques to monitor free oxide content in molten fluoride media, J. Electroanal. Chem. 606 (2007) 17–23.
[19] C.F. Baes Jr., The chemistry and thermodynamics of molten salt reactor fuels, J. Nucl. Mater. 51 (1974) 149–162.
[20] P. Chamelot, L. Massot, L. Cassayre, P. Taxil, Electrochemical behaviour of thorium(IV) in molten LiF-CaF2 medium on inert and reactive electrodes, Electrochim. Acta 55 (16) (2010) 4758–4764.
[21] F.R. Clayton, G. Mamantov, D.L. Manning, Electrochemical studies of uranium and thorium in molten LiF-NaF- KF at 500°C, J. Electrochem. Soc. 121 (1) (1974) 86.
[22] G. Mamantov, D.L. Manning, Voltammetry and related studies of uranium in molten lithium fluoride-beryllium fluoride-zirconium fluoride, Anal. Chem. 38 (11) (1966) 1494–1498.
[23] G.L. Fredrickson, G. Cao, P.K. Tripathy, M.R. Shaltry, S.D. Herrmann, T. Yoo, T.Y. Karlsson, D.C. Horvath, R. Gakhar, A.N. Williams, R.O. Hoover, W.C. Phillips, K.C. Marsden, Review—electrochemical measurements in molten salt systems: a guide and perspective, J. Electrochem. Soc. 166 (13) (2019) D645–D659.
[24] P. Souček, O. Beneš, A. Tosolin, R.J.M. Konings, Chemistry of molten salt reactor fuel salt candidates, Trans. Am. Nucl. Soc. 118 (1) (2018) 114–117.
[25] S. Pizzini, R. Morlotti, Oxygen and hydrogen electrodes in molten fluorides, Electrochim. Acta 10 (1965) 1033–1041.
[26] S. Mukherjee, S. Dash, S.K. Mukerjee, K.L. Ramakumar, *Thermodynamic investigations of* oxyfluoride of thorium and uranium", J. Nucl. Mater. 465 (2015) 604–614.
[27] V.I. Konstantinov, E.G. Polyakov, P.T. Stangrit, Cathodic processes at electrolysis of chloride fluoride ans oxyfluoride melts of niobium, Electrochim. Acta 26 (1981) 445–448.
[28] E. Christensen, X. Wang, J.H. von Barner, T. Ostfold, N.J. Bjerrum, The influence of oxide on the electrodeposition of niobium from alkali fluoride melts, J. Electrochem. Soc. 141 (5) (1994) 1212–1220.
[29] F. Lantelme, Y. Berghoute, J.H. von Barner, G.S. Picard, The influence of oxide on the electrochemical processes in K2NbF7-NaCl-KCl Melts, J. Electrochem. Soc. 142 (12) (1995) 4097–4102.
[30] P. Chamelot, B. Lafage, P. Taxil, Using square wave voltammetry to monitor molten alkaline fluoride baths for electrodeposition of niobium, Electrochim. Acta 43 (5–6) (1997) 607–616.
[31] V. Van, A. Silný, J. Hıνeš, V. Daněk, Electrochemical study of niobium fluoride and oxyfluoride complexes in molten LiF–KF–K2NbF7 bath, Electrochem. Commun. 1 (7) (1999) 295–300.
[32] C. Hamel, P. Chamelot, P. Taxil, Neodynium(III) cathodic processes in molten fluorides, Electrochim. Acta 49 (2004) 4467–4476.
[33] S. Delpech, S. Jaskierowicz, D. Rodrigues, Electrochemistry of thorium fluoride in LiCl-KCl eutectic melts and methodology for speciation studies with fluorides ion, Electrochim. Acta 144 (2014) 383–390.
[34] T. Berzins, P. Delahay, Oscillographic polarographic waves for the reversible deposition of metals on solid, J. Am. Chem. Soc. 75 (3) (1953) 555–559.
[35] C. Hamel, P. Chamelot, A. Laplace, E. Walle, O. Dugne, P. Taxil, Reduction process of uranium (IV) and uranium (III) in molten fluorides, Electrochim. Acta 52 (2007) 3995–4003.
[36] C. Nourry, P. Soucek, L. Massot, R. Malmbeck, P. Chamelot, J.P. Glatz, Electrochemistry of uranium in molten LiF-CaF2, J. Nucl. Mat. 430 (2012) 58–63.
[37] L. Cassayre, J. Serp, P. Soucek, R. Malmbeck, J. Rebizant, J.P. Glatz, Electrochemistry of thorium in LiCl-KCl eutectic melts, Electrochim. Acta 52 (26) (2007) 7432–7437.
[38] M. Gibilaro, L. Massot, P. Chamelot, *Thermodynamic properties determination in LiF-CaF2 using electrochemistry in high temperature fused salts: application to CeF3*", J. Electrochem. Soc. 164 (12) (2017) 307–311.
[39] S. Delpech, D. Rodrigues, G. Duran-Klie, Extraction of zirconium in the molten salt fast reactor, in: Proceedings of the ICAPP2019 Conference, Juan les Pins, France, 2019.
[40] M.W. Chase Jr., NIST-JANAF thermochemical tables fourth edition, Journal of

Physical and Chemical Reference Data, Monograph 9, American Chemical Society and American Institute of Physics, Washington, DC and New York, 1998.
[41] E. Capelli, O. Beneš, R.J.M. Konings, Thermodynamic assessment of the LiF–NaF-BeF2-ThF4-UF4 system, J. Nucl. Mater. 449 (2014) 111–121.
[42] S. Rouquette-Sanchez, G.S. Picard, Chalcogenide chemistry in molten salts. I. Selenium(IV) acido-basic and redox properties in the LiCl–KCl eutectic melt at 450, 500, 550 and 600°C, J. Electroanal. Chem. 572 (2004) 173.
[43] G. Durán-Klie, Étude du Comportement de L'uranium et de L'iode Dans le Mélange de Fluorures Fondus LiF-ThF4 à 650°C, University Paris-Saclay, Paris, 2017 thesis(in French) available online: https://tel.archives-ouvertes.fr/tel-01620474 (accessed April 2020).
[44] D. Rodrigues, Solvatation du Thorium Par les Fluorures en Milieu sel Fondu à Haute Température: Application au Procédé d'extraction Réductrice Pour le Concept MSFR, University Paris-Saclay, Paris, 2015 thesis(in French) available online: https://tel.archives-ouvertes.fr/tel-01250763 (accessed April 2020).
[45] S. Delpech, C. Cabet, C. Slim, G.S. Picard, Molten fluorides for nuclear applications, Mater. Today 13 (12) (2010) 34–41.
[46] M. Numakura, N. Sato, C. Bessada, Y. Okamoto, H. Akatsuka, A. Nezu, Y. Shimohara, K. Tajima, H. Kawano, T. Nakahagi, H. Matsuura, Structural investigation of thorium in molten lithium-calcium fluoride mixtures for salt treatment process in molten salt reactor, Prog. Nucl. Energy 53 (2011) 994–998.
[47] C. Bessada, D. Zanghi, M. Salanne, A. Gil-Martin, M. Gibilaro, P. Chamelot, L. Massot, A. Nezu, H. Matsuura, Investigation of ionic local structure in molten salt fast reactor LiF-ThF4-UF4 fuel by EXAFS experiments and molecular dynamics simulations, J. Mol. Liq. 307 (2020) 112927.